SOFT ROBOTICS
Volume 00, Number 00, 2022

DOI: 10.1089/soro.2021.0126

SoRo
Soft Robotics

Open camera or QR reader and scan code to access this article and other resources online.

Bioinspired Multimodal Multipose Hybrid Fingers for Wide-Range Force, Compliant, and Stable Grasping

Jiaqi Zhu,[1] Zhiping Chai,[1] Haochen Yong,[1] Yi Xu,[1] Chuanfei Guo,[2] Han Ding,[1] and Zhigang Wu[1]

Abstract

The increasing demand for grasping diverse objects in unstructured environments poses severe challenges to the existing soft/rigid robotic fingers due to the issues in balancing force, compliance, and stability, and hence has given birth to several hybrid designs. These hybrid designs utilize the advantages of rigid and soft structures and show better performance, but they are still suffering from narrow output force range, limited compliance, and rarely reported stability. Owing to its rigid-soft coupling structure with flexible switched multiple poses, human finger, as an excellent hybrid design, shows wide-range output force, excellent compliance, and stability. Inspired by human finger, we propose a hybrid finger with multiple modes and poses, coupled by a soft actuator (SA) and a rigid actuator (RA) in parallel. The multiple actuation modes formed by a pneumatic-based rigid-soft collaborative strategy can selectively enable the RA's high force and SA's softness, whereas the multiple poses derived from the specially designed underactuated RA skeleton can be flexibly switched with tasks, thus achieving high compliance. Such hybrid fingers also proved to be highly stable under external stimuli or gravity. Furthermore, we modularize and configure these fingers into a series of grippers with excellent grasping performance, for example, wide graspable object range (diverse from 0.1 g potato chips to 27 kg dumbbells for a 420 g two-finger gripper), high compliance (tolerate objects with 94% gripper span size and 4 cm offset), and high stability. Our study highlights the potential of fusing rigid-soft technologies for robot development, and potentially impacts future bionics and high-performance robot development.

Keywords: bioinspired finger, multiple modes, multiple poses, soft-rigid design, wide-range force, grasping

Introduction

Grasping is one of the most common and important actions of robotic fingers in interacting with the world. With a rapid increase in practical applications in recent years, efficient and stable grasping of diverse objects in complex unstructured environments has shown unprecedented importance and brought increasing challenges to the existing robotic fingers. Of particular, the soft ones, mainly composed of soft materials, show excellent compliance and softness, and are suitable for handling uncertain tasks, for example, grasping objects with unknown attributes,[1–8] with various actuation strategies.[9–14] Nevertheless, some issues also come along, for example, low stability, low upper limit of output force, and stiffness.

[1]Soft Intelligence Lab, State Key Laboratory of Digital Manufacturing Equipment and Technology, Huazhong University of Science and Technology, Wuhan, China.
[2]Department of Materials Science and Engineering, Southern University of Science and Technology, Shenzhen, China.

Introduction of variable stiffness mechanisms,[15–22] for example, granular jamming[15–17] and antagonistic arrangement,[19] can somehow improve the performance of these fingers without hindering their compliance and softness. However, their maximum load capacity is still far from that of the rigid or real ones. In contrast, the rigid fingers are usually powerful and stable, but when facing complex unstructured environments or uncertain tasks, for example, manipulating fragile objects, their inherent low compliance and high stiffness pose great challenges to sense and control.[23–28]

Recent attempts have been tried to couple rigid and soft structures and make them collaborate with each other to inherit their respective advantages,[29–32] for example, the high output force of the former and the softness of the latter. In these designs, a rigid-soft collaborative strategy, for example, ratchet controllable locking,[29] is usually needed to conditional weaken the influence of rigid structure, as the rigid ones are quite strong and can easily cover up the low forces of soft ones. Such hybrid designs are quite promising. For example, a bistable hybrid two-finger gripper can safely pick up a fragile egg and stably lift a 11.4 kg dumbbell.[30]

However, some challenges remain: (1) the existing rigid-soft collaborative strategies still cannot fully exploit the high force advantage of rigid structure without sacrificing the softness of soft one; (2) the relatively complex and bulky structure of existing hybrid fingers greatly limits their compliance to objects with varied attributes. In addition, high stability is also desired by robotic fingers, as the soft fingers are prone to deform or longtime vibrate under gravity or external stimuli,[33,34] for example, sharp speed changes and external impact, but the stability of hybrid fingers has rarely been studied.

Human finger is a natural hybrid design with wide-range output force, excellent compliance, and stability, Figure 1A. This mainly relies on its rigid-soft coupling compliant structure with flexibly switched multiple poses: the collaboration of tendons and phalanges enables it to output wide-range force, whereas the flexibly switched multiple poses of the phalanges bring it excellent compliance. In addition, thanks to the phalanges' restriction and the joints' damping, the human finger also shows high stability under gravity and external stimuli.

Inspired by human finger, in this study we present a hybrid finger with multimode and multipose to overcome the aforementioned issues, Figure 1. The finger is coupled in parallel by a rigid actuator (RA) based on an underactuated skeleton and a fiber-reinforced soft actuator (SA).[35,36] A pneumatic-based rigid-soft collaborative strategy was proposed to form four typical actuation modes, in which the RA's high force and SA's softness can be selectively fully highlighted, Figure 1B. The compact design can also well mimic the multiple poses of real finger owing to its specially designed underactuated skeleton, together with compliantly and flexibly switch its poses with tasks, Figure 1C. Moreover, the finger's hybrid structure proved to be highly stable under gravity and external stimuli.

We introduced the finger's design and implementation, systematically studied its output force and stability, and finally demonstrated its performance by modularizing and assembling it into a series of grippers with excellent grasping performance, for example, wide-range graspable objects (Fig. 1D), high compliance, and high stability. Such hybrid fingers with rich gripper configurations can be used in multiple fields, for example, human–robot interaction,[37,38] industrial sorting,[2] biological sample collection,[39] and food processing,[40] in the future.

Design and Implementation

Multiple modes

Our hybrid finger consists of an RA and an SA in parallel, both of which are pneumatic. The RA is an underactuated skeleton actuated by a piston, whereas the SA is a soft bending actuator. They can be actuated independently or cooperatively, forming the following four actuation modes for different scenarios, Figure 1B:

1. When the finger needs to maintain or restore to its initial state, a high negative pressure P_3 is introduced into the syringe of RA, whereas the SA is connected to the atmosphere. During this process, RA dominates.
2. When the finger needs to manipulate fragile and lightweight objects, for example, potato chips and strawberries, SA needs to dominate. An offset air pressure P_f is introduced into the syringe to balance the piston friction f (the determination of the offset air pressure is in Section S1 of the Supplementary Data and Supplementary Figs. S1 and S2), so that the piston can be pulled by a slight force from the SA (the bending performance of the finger in this mode is in Section S2 of the Supplementary Data and Supplementary Figs. S3 and S4). In this mode, the finger is approximately equivalent to an ordinary pneumatic soft finger.
3. When the finger needs to grasp and lift some rigid and heavy objects, for example, dumbbells, RA can dominate. A high positive pressure P_2 is passed into the syringe, whereas the SA is connected to the atmosphere. At this time, the finger is equivalent to an underactuated pneumatic finger with high output force and response speed.
4. The two actuators can also cooperate temporally to pick up some heavier but fragile objects. For example, when the finger needs to grasp a piece of 450 g tofu, SA itself cannot provide sufficient force to lift it, whereas directly actuating the fast and powerful RA in mode 3 will easily damage the tofu. Therefore, the SA can be actuated first in mode 2 to gently touch the tofu, and then the RA can be actuated to provide sufficient force. Such a collaborative strategy can also be applied to other target objects with similar characteristics, for example, a bunch of grapes, and a cup of water that is easily knocked over. In addition, when the pressure of RA is difficult to be further increased, SA can also be actuated after RA to further increase the total output force of the finger in a small range.

Multiple poses

As shown in Figure 1C, besides the embracing pose, the human finger can also stabilize in other four distal phalanx press poses under forces from different directions. These poses can be flexibly switched along different tasks, bringing

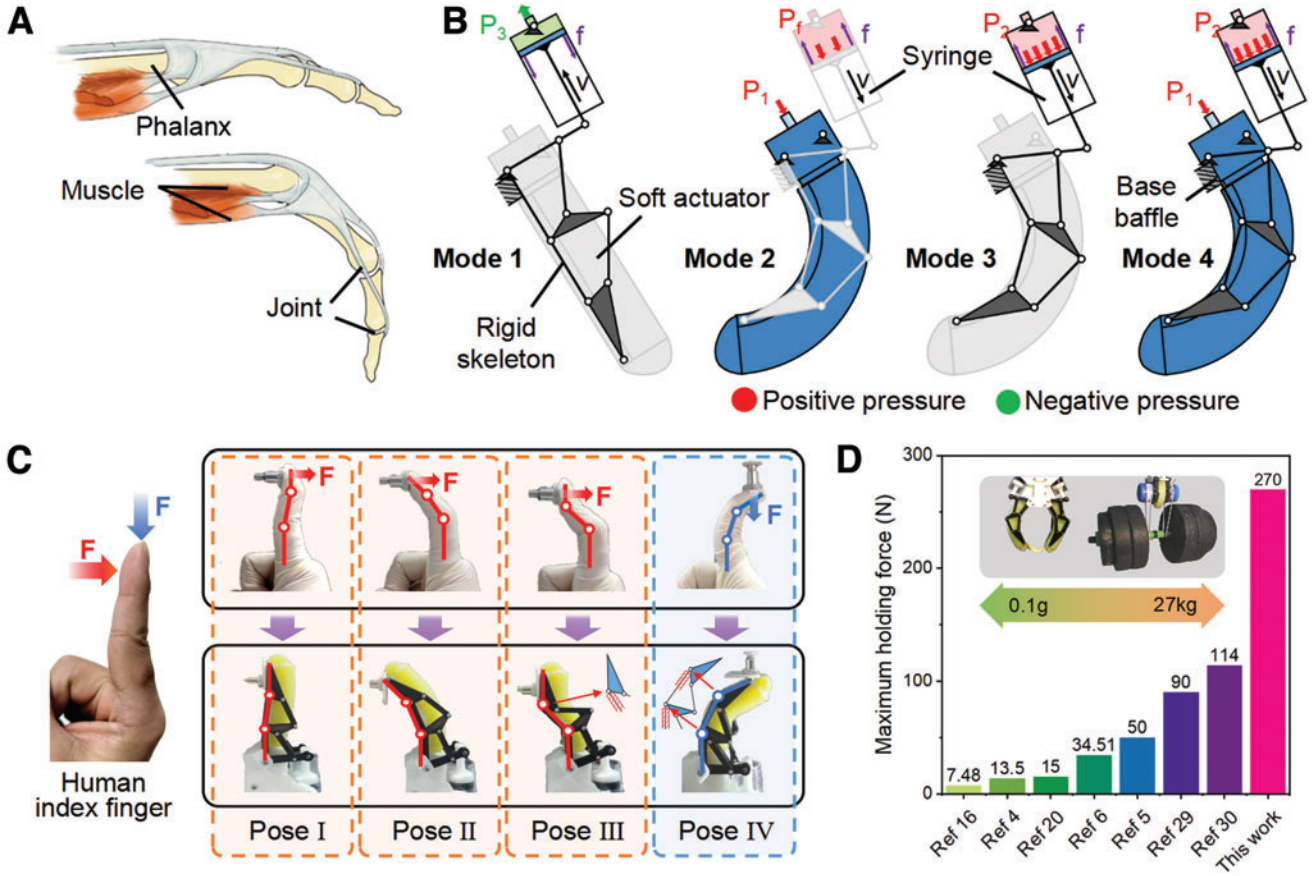

FIG. 1. Bioinspired multimodal multipose hybrid fingers. **(A)** Schematic diagram of the rigid-soft coupling structure of human finger. **(B)** Structures and four typical actuation modes of the proposed hybrid finger (the *dark color* indicates the dominant part, whereas the *light gray* indicates the slave). **(C)** The hybrid finger can well mimic the multiple poses of human finger, among which the poses I to IV are the back Z pose, forward pose, front Z pose, and reclining pose, respectively. **(D)** The maximum holding force of a two-finger gripper based on the proposed finger has far exceeded the current finger-based soft/hybrid grippers. Color images are available online.

high compliance without sacrificing the finger's high force output. Unfortunately, so far, these poses are neglected in most of the bionic robotic finger designs.[41–45]

To mimic the multiple poses of human finger, first, we adopt an underactuated mechanism as the rigid skeleton, through whose uncontrolled degrees of freedom the finger can already imitate the compliant embracing of real one. Then, we set a base baffle at the proximal phalanx to help transmit the driving force to the distal phalanx, and thus the finger can achieve powerful press in the first two distal phalanx press poses: pose I (back Z pose) and II (forward pose), Figure 1B. The latter two distal phalanx press poses are somewhat difficult to mimic as they involve the over-travel locking mechanism of the finger joints.

Considering this, we set baffles on the proximal and middle phalanx connecting rods of underactuated skeleton to make the triangle plates stuck when over-rotating reversely (Supplementary Fig. S5), so that the hybrid finger can also mimic the remaining two distal phalanx press poses: pose III (front Z pose) and IV (reclining pose). The formation of these poses and a statics model of the finger in various poses can be found in Sections S3 and S4 of the Supplementary Data and Supplementary Figures S6–S9.

Such multiple bionic poses can endow the hybrid finger with excellent compliance without sacrificing its wide output force range in each pose, as further demonstrated hereunder.

Structural design

The structure of the finger is soft-rigid coupled, where the SA and RA with independent air paths are connected in parallel by bolts, Figure 2A–C. The main body of the SA adopts fiber-reinforced design for limiting radial deformation during expansion.[35,36] Its one end is bonded with a fixed part, and the other end is bonded with a softer fingertip. Several through holes are distributed on the inextensible layer for parallel connections, Figure 2D and E. The RA consists of an underactuated skeleton and a piston mechanism (Supplementary Fig. S10A), which are hinged at the distal end of the piston rod by a steel shaft for force transmission. The syringe of the piston mechanism is then hinged with the base through cylindrical protrusions on both sides of its outer wall.

The setting of the soft fingertip can prevent the rigid skeleton from touching and hence damaging fragile objects in the forward pose, whereas a similar situation can be avoided in other poses by thickening the inextensible layer of SA to assure the soft parts touch the objects first. The material

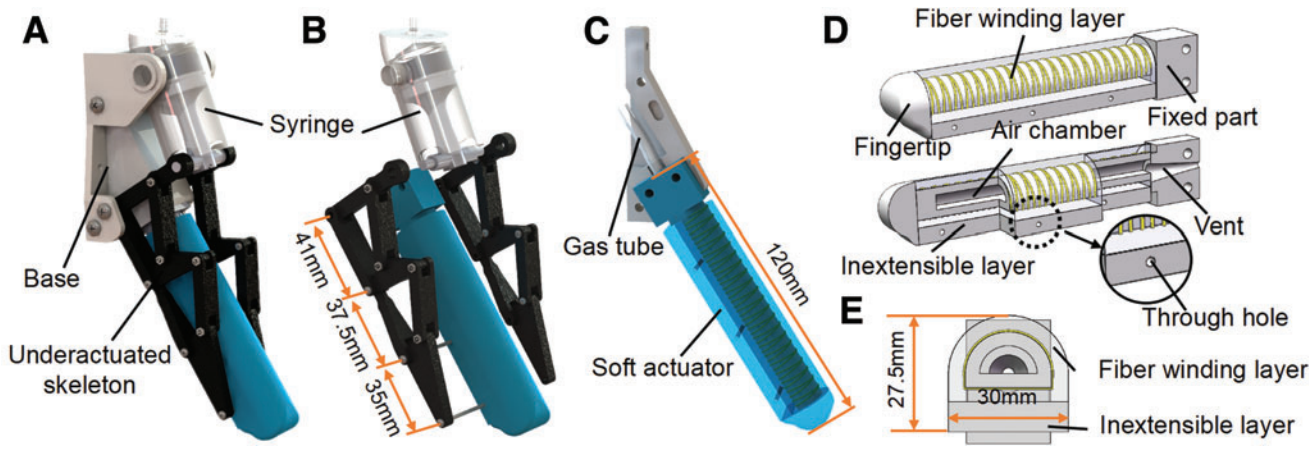

FIG. 2. Structural design of the hybrid finger. **(A)** The proposed hybrid finger. **(B)** Exploded diagram of rigid actuator. **(C)** Installation of soft actuator. **(D)** Internal structure diagram of soft actuator. **(E)** Sectional view of soft actuator. Color images are available online.

selection and fabrication process of the whole finger and corresponding pneumatic control system can be found in Sections S5 and S6 of the Supplementary Data and Supplementary Figures S10–S12.

Results and Discussion

Output force in multiple poses

We first studied the embracing force of the fingers through an extension method. During the tests, the finger was actuated to wrap a cylinder, and a force gauge rose at 5 mm/s to gradually pull the cylinder away from the finger and record the force changes (the setup is in Supplementary Fig. S13). The RA tests were conducted in mode 3, whereas the SA tests were performed by removing the piston mechanism (a finger without piston mechanism proved to have close output force as a finger in mode 2 in specific embracing poses, Supplementary Fig. S14). As shown in Figure 3A and B, we found that the embracing force of RA is inversely proportional to the object's size, and directly proportional to the air pressure. The force can reach 210.74 N at 350 kPa when embracing a 40 mm cylinder, which is high enough to compare with most motor-based rigid fingers.[27,46]

By increasing the air pressure or reducing the object's size continuously, the embracing force of RA can be further increased. In contrast, the embracing force of SA seems to have no obvious relationship with the object's size, although it increased with the increasing pressure, Figure 3C and D. The force can reach 5.78 N at 50 kPa by embracing a 40 mm cylinder. Another finding is that there was a clear force drop during the SA's tests, regardless of the object size being embraced. We found that this might be caused by the gradual pose transition of SA from embracing to distal phalanx press pose as the extension increases. We also calculated the output force resolution of the two actuators by linear fitting the pressure versus force figures, Figure 3B and D. The higher resolution of SA allows the finger to better control its output force in mode 2 to safely grasp fragile objects.

We then evaluated the finger output force in the distal phalanx press poses. The RA's performance was tested in mode 3, whereas the SA's performance was tested in mode 2 (the setups and shots are in Supplementary Fig. S15). The calculated theoretical curves were plotted for reference. As shown in Figure 3E, there is a linear relationship between the output force and the input air pressure of RA in all four distal phalanx press poses, and the finger output force is the largest in the front Z pose (reach a considerable high force of 101.65 N at 420 kPa) and the smallest in the back Z pose under certain air pressure. The theoretical curves fit well with the experimental ones in all three poses except the reclining pose, and the deviations are mainly caused by the elastic deformation of connecting rods.

The relatively large deviation in reclining pose indicates the poor deformation resistance of the rigid skeleton in this pose, which is similar to human finger. The front Z pose and the reclining pose are two conditional poses, both of which require a certain initial force to generate as the triangle plates need to overcome the SA's bending moments to contact baffles, which is also similar to our finger.

For SA, there is a positive correlation between the output force and the input pressure in the forward and back Z poses, Figure 3F. In the forward pose, the SA needs a certain initial air pressure to bend and contact the object before generating output force. The SA's output force is quite low compared with RA, with an average force of only 3.43 N at 50 kPa in the two poses.

In addition, we also conducted experiments to study the output force of the finger in mode 4. In this mode, both actuators were actuated and the output force was their superposition result. The results show that the finger's output force in mode 4 is slightly deviated from the sum of the two actuators' respective output force in modes 2 and 3. The deviation might be caused by the coupling relationship between the output force of RA and SA (see Section S7 of the Supplementary Data and Supplementary Fig. S16 for details).

Stability tests

To evaluate the stability of the hybrid finger, tests were conducted with a high-speed camera under three typical

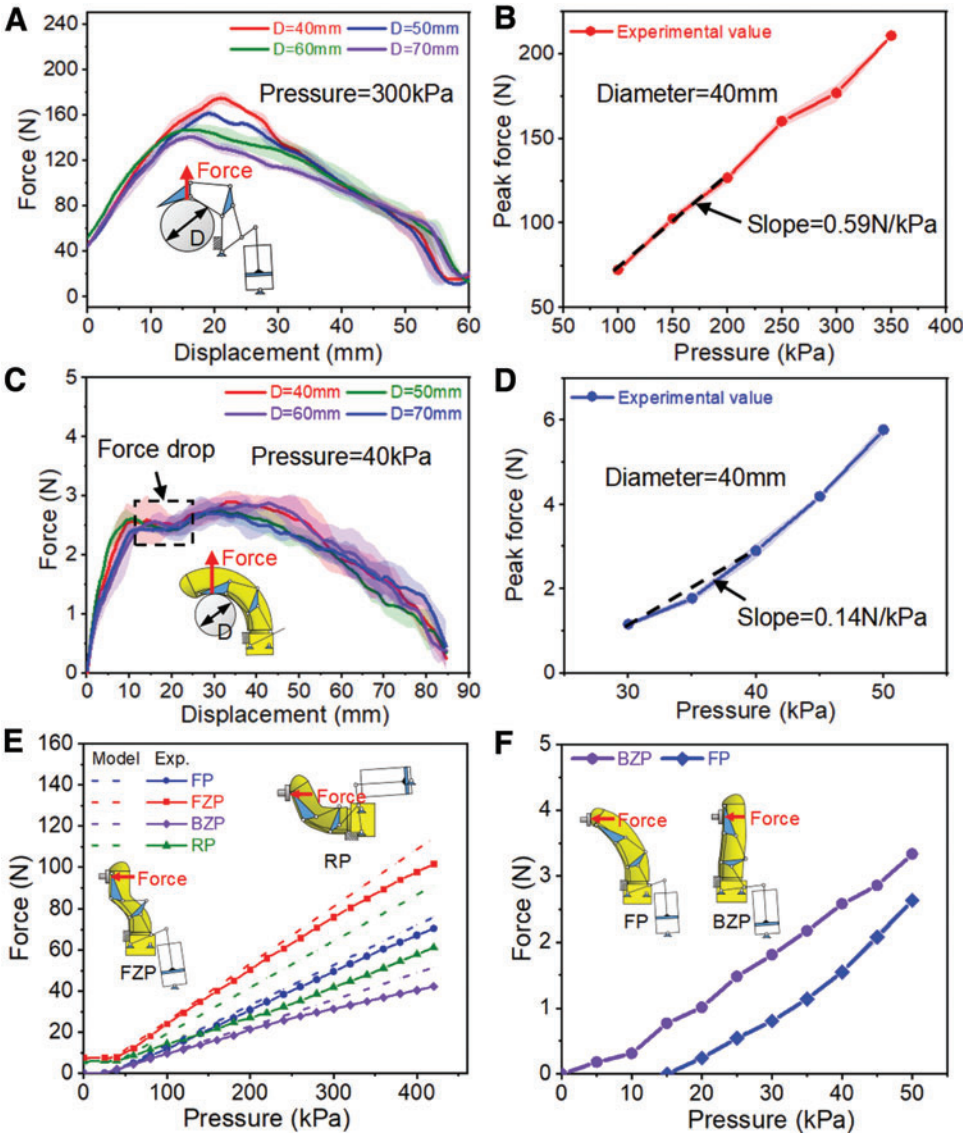

FIG. 3. Output force tests of the hybrid finger in multiple poses. **(A)** Object's size versus output force of the rigid actuator in embracing pose. **(B)** Input air pressure versus peak force of the rigid actuator in embracing pose. **(C)** Object's size versus output force of the soft actuator in embracing pose. **(D)** Input air pressure versus peak force of the soft actuator in embracing pose. **(E)** Input air pressure versus output force of the rigid actuator in four distal phalanx press poses: FP, FZP, BZP, and RP. **(F)** Input air pressure versus output force of the soft actuator in FP and BZP. BZP, back Z pose; FP, forward pose; FZP, front Z pose; RP, reclining pose. Color images are available online.

working conditions: (1) sudden impacts, (2) sharp speed changes, and (3) changed gravity direction. A fully soft finger was used for comparison.

We first performed the sudden impact tests by knocking the two fingers simultaneously from both sides with a hammer handle. The compliant deformation process of the hybrid finger can be seen in Figure 4A and B. The results reveal that the hybrid finger can recover quickly within 0.5 s at a much smaller amplitude than the soft one, Figure 4C and D. In this process, the SA can damp the influence of the impact, and simultaneously the rigid joint damping can quickly weaken the amplitude. It should be noted that in the current version, the hybrid finger still cannot deform compliantly under impact perpendicular to its symmetry plane. To solve this, also inspired by human finger, we intend to introduce an extra swing degree of freedom near the proximal joint of the hybrid finger in our future versions.

We then conducted the sharp speed change tests by using a linear module to carry two fingers to travel a certain distance at different speeds and suddenly stop. The results shown in Figure 4E and F reveal that the hybrid finger had almost no visible vibration at all measured speed changes, which may owe to the rigid skeleton's restriction and the rigid joint static friction, whereas the amplitudes of the soft finger were proportional to the speed changes and usually took a few seconds to subside.

Finally, we performed the changed gravity direction tests by letting the two fingers deform freely under two typical gravity directions. The results show that the hybrid finger can well maintain its initial shape under changed gravity direction, whereas the soft finger had obvious drooping phenomenon, with a fingertip vertical offset of 15.63 mm (14% body length) and 4.46 mm (4% body length), respectively, Figure 4G and H.

The aforementioned tests well prove the high stability of the hybrid finger under various external stimuli and gravity, which is conducive to its efficient and precise work in complex unstructured environments.

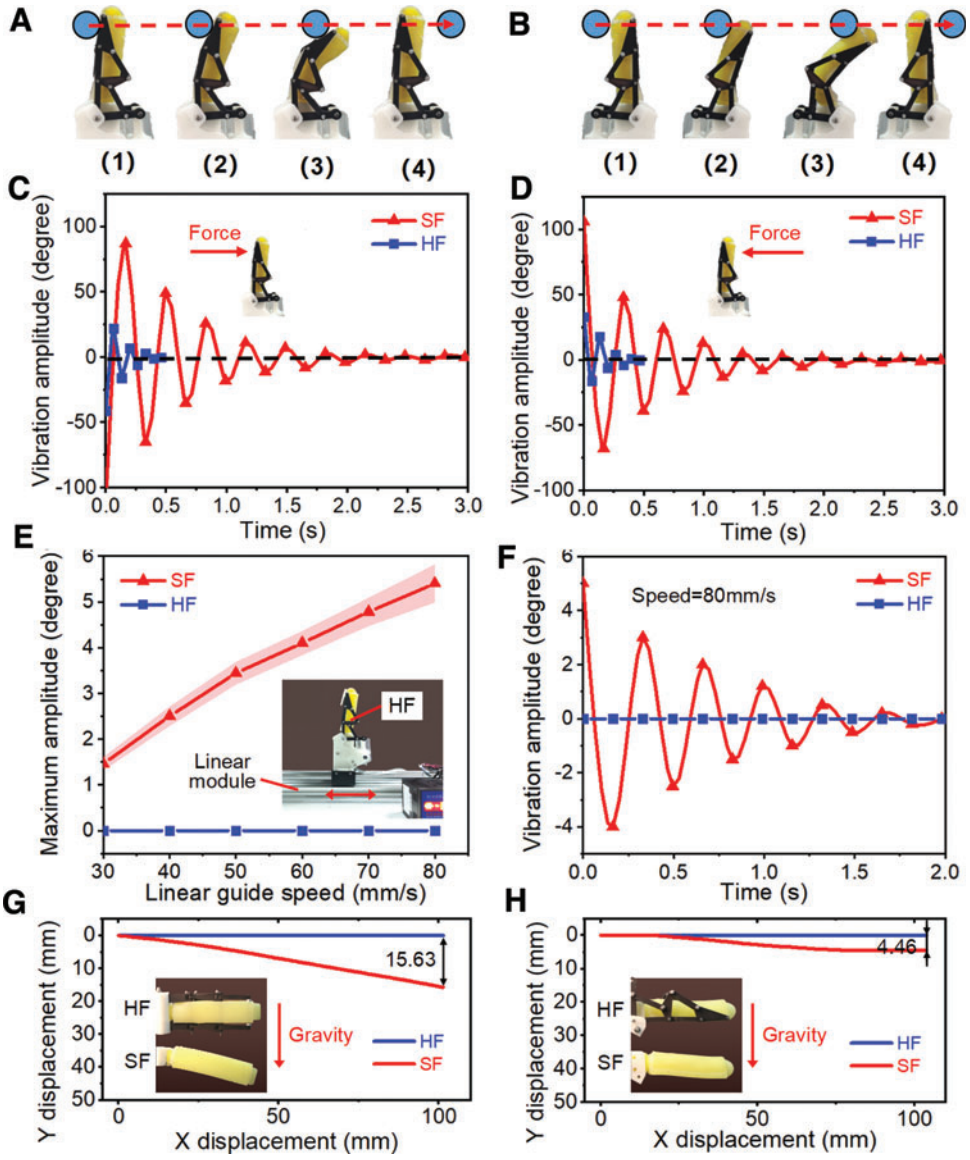

FIG. 4. Stability tests of the HF and the SF under external impact, sharp speed changes, and gravity. **(A)** Deformation of HF under a front-side impact. **(B)** Deformation of HF under a back-side impact. **(C)** Vibration dissipation process of two fingers under a front-side impact. **(D)** Vibration dissipation process of two fingers under a back-side impact. **(E)** The maximum amplitude of two fingers under different speed changes. **(F)** Vibration dissipation process of two fingers at 80 mm/s speed change. **(G)** Deformation of two fingers under gravity perpendicular to their symmetry plane. **(H)** Deformation of two fingers under gravity parallel to their symmetry plane. HF, hybrid finger; SF, soft finger. Color images are available online.

Grasping performance

To further demonstrate the finger performance, we modularized and assembled these hybrid fingers into a series of grippers through some frames (Section S8 of the Supplementary Data and Supplementary Figs. S17 and S18). The grasping performance of the grippers was evaluated by grasping some representative objects with various attributes. Each grasping involves a complete pick-and-drop process with at least several seconds stable holding time.

The first explored performance is the graspable objects range. By flexibly switching between four modes, the RA's high force and SA's softness can be selectively fully highlighted, and a simple 420 g two-finger gripper can not only safely grasp a piece of potato chip, a strawberry, a piece of jelly, but also can stably lift a 27 kg dumbbell (Fig. 5A and Supplementary Movie S1). Its maximum holding force has far exceeded the current finger-based soft/hybrid grippers (Fig. 1D), whereas its maximum load-to-weight ratio of 6429% is also highly competitive among centimeter-scale grippers (Supplementary Table S1).

Complementary, a three-fingered circular gripper was assembled to grasp some large objects with approximately cylindrical or spherical outlines, for example, a balloon, or a wide edge bowl, whereas a three-finger interlaced gripper was used to grasp some slender objects, for example, a cabbage, or a solid steel shaft, Figure 5B and C. These flexibly switchable configurations can greatly enrich the overall application scope.

High compliance is another important feature of our grippers (Supplementary Movie S2). The multiple poses of the hybrid fingers can be flexibly switched with different tasks, thus greatly enhancing the compliance without sacrificing the finger's high force output. Specifically, the fingers will naturally utilize the forward pose when pinching some small and lightweight objects in mode 2, for example, a piece of 0.1 mm thick paper, Figure 6A. When grasping objects in mode 3 or 4, the fingers may jump to the front Z pose, under which a higher and more stable output force can be obtained, Figure 6B. When grasping some wide objects, for example, a 15.5 cm wide box (about 94% of the gripper

FIG. 5. Wide graspable objects range of the series of grippers. **(A)** A two-finger gripper can grasp a range of objects from fragile and lightweight to heavy and rigid. The first line from *left* to *right*: a piece of potato chip (1 g), a strawberry (25 g), a banana (137 g), a bread (155 g), a piece of jelly (200 g), and a piece of tofu (450 g). The second line from *left* to *right*: a section of aluminum alloy profile (1.35 kg), a bottle of laundry detergent (3.95 kg), a motor (6 kg), and a dumbbell (27 kg). **(B)** A three-finger circular gripper can grasp a balloon (1 g), a wide edge bowl (150 g), a cauliflower (210 g), and half bucket of water (5.3 kg). **(C)** A three-finger interlaced gripper can grasp a cabbage (300 g), a linear module (3.6 kg), and a solid steel shaft (7.9 kg). Color images are available online.

span), the fingers can compliantly adapt to the shape and stably pinch the objects in the back Z pose, Figure 6C.

The fingers can also flexibly transform into the reclining pose when being pressed on a heavy object and dragging it to move, Figure 6D. In addition, the high compliance can also be reflected in grasping objects with high offsets. As shown in Figure 6E and F, when grasping some heavy or fixed objects with 4 cm offset, the fingers can be compliantly deformed to the suitable poses, for example, one in forward pose and the other in back Z pose, and stably pinch them. However, when the grasped object is lightweight, the fingers will push it to the approximate centering position and then pinch it. For the latter case, experiments were conducted, and the results show that a two-finger gripper can still stably grasp samples offsetting up to 78% of the gripper span (Section S9 of the Supplementary Data and Supplementary Fig. S19).

These grippers also show high stability when performing tasks. They not only share high accuracy and grasping force in all grasping directions, which further enriches their application range (Fig. 6G–J), but also can quickly stabilize under sudden speed changes and impacts (Supplementary Movie S3).

Conclusion

In brief, we developed a bioinspired hybrid finger with multiple modes and poses, coupled by an RA and an SA in parallel. Its multiple actuation modes formed by pneumatic-based rigid-soft collaborative strategy can selectively fully highlight the RA's high force and SA's softness, whereas its bioinspired multiple poses can be flexibly switched with varied tasks, thus bringing high compliance. Also, the finger's hybrid structure proved to be highly stable under gravity and external stimuli.

Based on these fingers, a series of grippers with different configurations can be easily assembled. All of them show excellent grasping performance, for example, wide graspable objects range (from 0.1 g potato chips to a 27 kg dumbbell for a 420 g two-finger gripper), high grasping

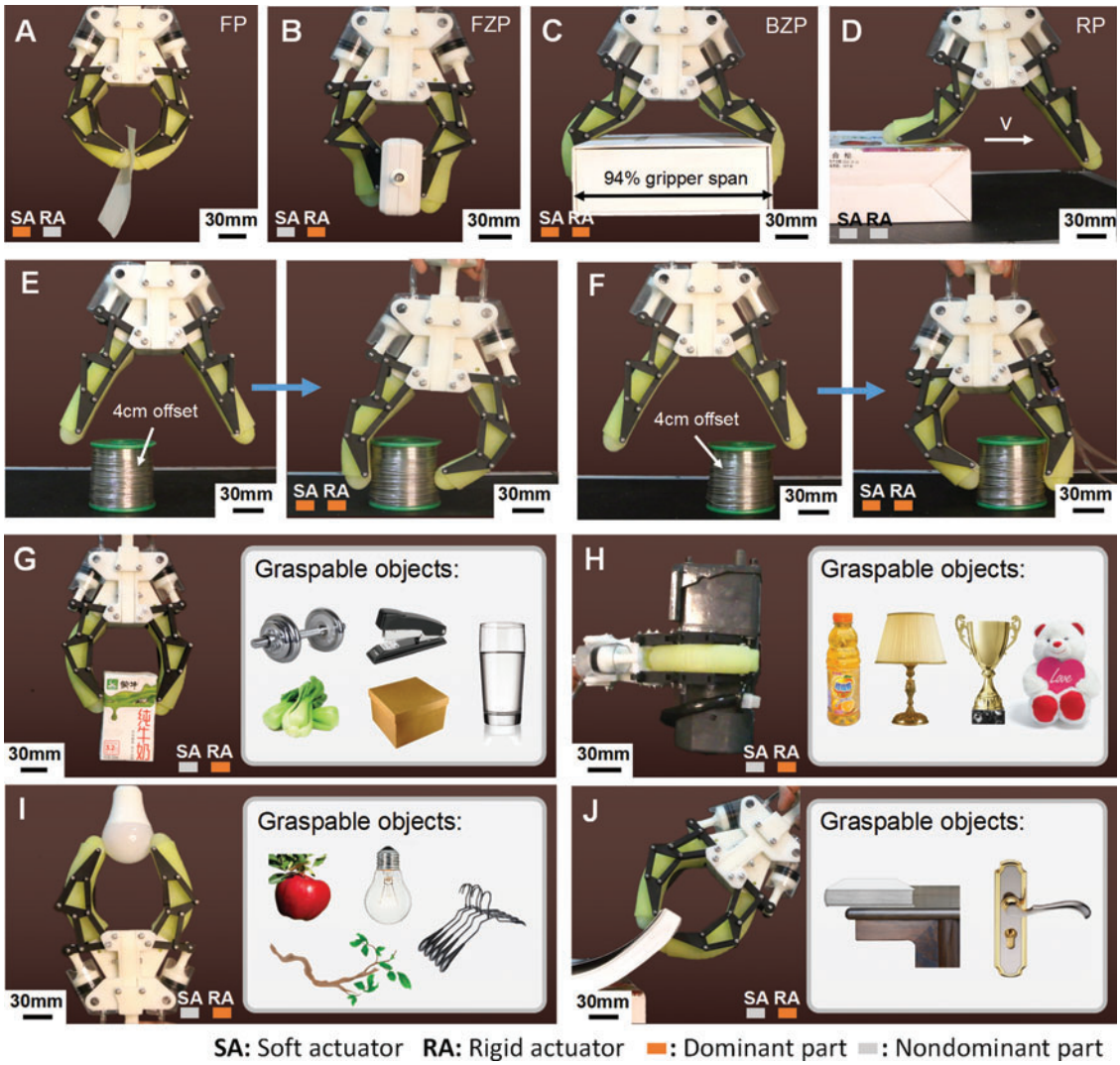

FIG. 6. High grasping compliance and stability of the series of grippers demonstrated by a two-finger gripper. **(A)** Grasping a piece of paper (1 g) in the forward pose. **(B)** Grasping a force gauge (250 g) in the front Z pose. **(C)** Grasping a wide box (550 g) in the back Z pose. **(D)** Dragging a box of 3D printing wire (1.05 kg) in the reclining pose. **(E)** Grasping a roll of Sn-0.7Cu wire (850 g) 4 cm off the center line to the *left*. **(F)** Grasping a roll of Sn-0.7Cu wire (850 g) 4 cm off the center line to the *right*. **(G)** *Top* to *down* grasping a carton of milk (269 g). **(H)** *Horizontal* grasping a heavy motor (6 kg). **(I)** *Down* to *top* grasping a light bulb (80 g). **(J)** *Lateral* grasping a book (450 g). Color images are available online.

compliance (tolerate objects with 94% gripper span size and 4 cm offset), and high stability under gravity and external stimuli.

This study can provide a useful reference for subsequent research on bionic fingers and high-performance robot development, and some potential application fields of these grippers include human–robot interaction, industrial sorting, biological sample collection, and food processing.

Authors' Contributions

Z.W. supervised the research and edited the article. J.Z. conceived the concept, designed and iterated the prototypes, built the models, designed the experiments, and drafted the article. J.Z. and Z.C. performed the simulations. J.Z. and H.Y. carried out the experiments and data processing. J.Z., Z.C., H.Y., and Y.X. analyzed the data and interpreted the results. All authors contributed to the discussion.

Author Disclosure Statement

No competing financial interests exist.

Funding Information

The materials based on the study were partly financially supported by National Natural Science Foundation of China (Grant Nos. 52188162 and U1613204), National Key R&D program of China (Grant No. 2017YFB1303100), and Guangdong Innovative and Entrepreneurial Research Team Program under contract No. 2016ZT06G587.

Supplementary Material

Supplementary Data S1
Supplementary Movie S1
Supplementary Movie S2
Supplementary Movie S3

References

1. Shintake J, Cacucciolo V, Floreano D, *et al.* Soft robotic grippers. Adv Mater 2018;30:1707035.
2. Tawk C, Gillett A, in het Panhuis M, *et al.* A 3D-printed omni-purpose soft gripper. IEEE Trans Robot 2019;35: 1268–1275.
3. Langowski JKA, Sharma P, Shoushtari AL. In the soft grip of nature. Sci Robot 2020;5:eabd9120.
4. Hao Y, Gong Z, Xie Z, *et al.* Universal soft pneumatic robotic gripper with variable effective length. In: Chinese Control Conference (CCC). Chengdu, China: IEEE, 2016: 6109–6114.
5. Yap HK, Ng HY, Yeow CH. High-force soft printable pneumatics for soft robotic applications. Soft Robot 2016; 3:144–158.
6. Manti M, Hassan T, Passetti G, *et al.* A bioinspired soft robotic gripper for adaptable and effective grasping. Soft Robot 2015;2:107–116.
7. Subramaniam V, Jain S, Agarwal J, *et al.* Design and characterization of a hybrid soft gripper with active palm pose control. Int J Robot Res 2020;39:1668–1685.
8. Lee K, Wang Y, Zheng C. Twister hand: underactuated robotic gripper inspired by origami twisted tower. IEEE Trans Robot 2020;36:488–500.
9. Lau GK, Heng KR, Ahmed AS, *et al.* Dielectric elastomer fingers for versatile grasping and nimble pinching. Appl Phys Lett 2017;110:182906.
10. Xie Z, Domel AG, An N, *et al.* Octopus arm-inspired tapered soft actuators with suckers for improved grasping. Soft Robot 2020;7:639–648.
11. Zhu J, Lyu L, Xu Y, *et al.* Intelligent soft surgical robots for next-generation minimally invasive surgery. Adv Intell Syst 2021;3:2100011.
12. Yang Y, Vella K, Holmes DP. Grasping with kirigami shells. Sci Robot 2021;6:eabd6426.
13. Kellaris N, Rothemund P, Zeng Y, *et al.* Spider-inspired electrohydraulic actuators for fast, soft-actuated joints. Adv Sci 2021;8:2100916.
14. Wang W, Yu CY, Abrego Serrano PA, *et al.* Shape memory alloy-based soft finger with changeable bending length using targeted variable stiffness. Soft Robot 2020;7:283–291.
15. Yang Y, Zhang Y, Kan Z, *et al.* Hybrid jamming for bioinspired soft robotic fingers. Soft Robot 2020;7:292–308.
16. Wei Y, Chen Y, Ren T, *et al.* A novel, variable stiffness robotic gripper based on integrated soft actuating and particle jamming. Soft Robot 2016;3:134–143.
17. Brown E, Rodenberg N, Amend J, *et al.* Universal robotic gripper based on the jamming of granular material. Proc Natl Acad Sci U S A 2010;107:18809–18814.
18. Shintake J, Schubert B, Rosset S, *et al.* Variable stiffness actuator for soft robotics using dielectric elastomer and lowmelting-point alloy. In: IEEE/RSJ International Conference on Intelligent Robots and Systems (IROS). Hamburg, Germany: IEEE, 2015:1097–1102.
19. Nasab AM, Sabzehzar A, Tatari M, *et al.* A soft gripper with rigidity tunable elastomer strips as ligaments. Soft Robot 2017;4:411–420.
20. Zhang YF, Zhang N, Hingorani H, *et al.* Fast-response, stiffness-tunable soft actuator by hybrid multimaterial 3D Printing. Adv Funct Mater 2019;29:1806698.
21. Zhuo S, Zhao Z, Xie Z, *et al.* Complex multiphase organohydrogels with programmable mechanics toward adaptive soft-matter machines. Sci Adv 2020;6:eaax1464.
22. Yang Y, Chen Y, Li Y, *et al.* Novel variable-stiffness robotic fingers with built-in position feedback. Soft Robot 2017;4:338–352.
23. Hang K, Bircher WG, Morgan AS, *et al.* Manipulation for self-Identification, and self-Identification for better manipulation. Sci Robot 2021;6:eabe1321.
24. Jinda C, Jeff T. Toward next-generation learned robot manipulation. Sci Robot 2021;6:eabd9461.
25. Rodriguez A. The unstable queen: uncertainty, mechanics, and tactile feedback. Sci Robot 2021;6:eabi4667.
26. Yan Y, Hu Z, Yang Z, *et al.* Soft magnetic skin for super-resolution tactile sensing with force self-decoupling. Sci Robot 2021;6:eabc8801.
27. Laffranchi M, Boccardo N, Traverso S, *et al.* The Hannes hand prosthesis replicates the key biological properties of the human hand. Sci Robot 2020;5:eabb0467.
28. Xiong CH, Chen WR, Sun BY, *et al.* Design and implementation of an anthropomorphic hand for replicating human grasping functions. IEEE Trans Robot 2016;32: 652–671.
29. Guo XY, Li WB, Gao QH, *et al.* Self-locking mechanism for variable stiffness rigid-soft gripper. Smart Mater Struct 2020;29:035033.
30. Tang Y, Chi Y, Sun J, *et al.* Leveraging elastic instabilities for amplified performance: spine-inspired high-speed and high-force soft robots. Sci Adv 2020;6:eaaz6912.
31. Hu Q, Huang H, Dong E, *et al.* A bioinspired composite finger with self-locking joints. IEEE Robot Autom Lett 2021;6:1391–1398.
32. Liu X, Zhao Y, Geng D, *et al.* Soft humanoid hands with large grasping force enabled by flexible hybrid pneumatic actuators. Soft Robot 2021;8:175–185.
33. Li Y, Chen Y, Li Y. Pre-charged pneumatic soft gripper with closed-loop control. IEEE Robot Autom Lett 2019;4: 1402–1408.
34. Li Y, Chen Y, Ren T, *et al.* Precharged pneumatic soft actuators and their applications to untethered soft robots. Soft Robot 2018;5:567–575.
35. Polygerinos P, Wang Z, Overvelde JT, *et al.* Modeling of soft fiber-reinforced bending actuators. IEEE Trans Robot 2015;31:778–789.
36. Galloway KC, Polygerinos P, Walsh CJ, *et al.* Mechanically programmable bend radius for fiber-reinforced soft actuators. In: IEEE International Conference on Advanced Robotics. Montevideo, Uruguay: IEEE, 2013;1–6.
37. Chen S, Pang Y, Cao Y, *et al.* Soft robotic manipulation system capable of stiffness variation and dexterous operation for safe human-machine interactions. Adv Mater Technol 2021;6:2100084.
38. Chen S, Pang Y, Yuan H, *et al.* Smart soft actuators and grippers enabled by self-powered tribo-skins. Adv Mater Technol 2020;5:1901075.
39. Galloway KC, Becker KP, Phillips B, *et al.* Soft robotic grippers for biological sampling on deep reefs. Soft Robot 2016;3:23–33.
40. Wang Z, Kanegae R, Hirai S. Circular shell gripper for handling food products. Soft Robot 2021;8;542–554.
41. Kashef SR, Amini S, Akbarzadeh A. Robotic hand: a review on linkage-driven finger mechanisms of prosthetic hands and evaluation of the performance criteria. Mech Mach Theory 2020;145:103677.

42. Lee DH, Park JH, Park SW, *et al.* KITECH-hand: a highly dexterous and modularized robotic hand. IEEE/ASME Trans Mech 2017;22:876–887.
43. Zhang Z, Han T, Pan J, *et al.* Design of anthropomorphic fingers with biomimetic actuation mechanism. IEEE Robot Autom Lett 2019;4:3465–3472.
44. Zhou J, Chen X, Chang U, *et al.* A soft-robotic approach to anthropomorphic robotic hand dexterity. IEEE Access 2019;7:101483–101495.
45. Weiner P, Starke J, Hundhausen F, *et al.* The KIT prosthetic hand: design and control. In: IEEE/RSJ International Conference on Intelligent Robots and Systems (IROS). Madrid, Spain: IEEE, 2018:3328–3334.
46. Belter JT, Segil JL, Dollar AM, *et al.* Mechanical design and performance specifications of anthropomorphic prosthetic hands: a review. JRRD 2013;50:599–618.

Address correspondence to:
Zhigang Wu
Soft Intelligence Lab
State Key Laboratory of Digital Manufacturing Equipment and Technology
Huazhong University of Science and Technology
Wuhan 430074
China

E-mail: zgwu@hust.edu.cn